Rapid Communications | Editors' Suggestion

Decoupling spin-orbital correlations in a layered manganite amidst ultrafast hybridized charge-transfer band excitation

L. Shen,[1,2,*] S. A. Mack,[2,3] G. Dakovski,[2] G. Coslovich,[2] O. Krupin,[2] M. Hoffmann,[2] S.-W. Huang,[4,5] Y-D. Chuang,[4] J. A. Johnson,[6,7] S. Lieu,[2] S. Zohar,[2] C. Ford,[2] M. Kozina,[2] W. Schlotter,[2] M. P. Minitti,[2] J. Fujioka,[8,9] R. Moore,[1] W-S. Lee,[1] Z. Hussain,[4] Y. Tokura,[8,10] P. Littlewood,[11] and J. J. Turner[1,2,†]

[1]*Stanford Institute for Materials and Energy Sciences, Stanford University and SLAC National Accelerator Laboratory, Menlo Park, California 94025, USA*

[2]*Linac Coherent Light Source, SLAC National Accelerator Laboratory, Menlo Park, California 94025, USA*

[3]*Department of Physics, University of California, Berkeley, California 94720, USA*

[4]*Advanced Light Source, Lawrence Berkeley National Laboratory, Berkeley, California 94720, USA*

[5]*MAX IV Laboratory, Lund University, P. O. Box 118, 22100 Lund, Sweden*

[6]*Swiss Light Source, Paul Scherrer Institut (PSI), 5232 Villigen PSI, Switzerland*

[7]*Department of Chemistry and Biochemistry, Brigham Young University, Provo, Utah 84602, USA*

[8]*Department of Applied Physics and Quantum-Phase Electronics Center (QPEC), University of Tokyo, Hongo, Tokyo 113-8656, Japan*

[9]*Graduate School of Pure and Applied Science, University of Tsukuba, Tsukuba, Ibaraki 305-8573, Japan*

[10]*RIKEN Center for Emergent Matter Science (CEMS), Wako 351-0198, Japan*

[11]*James Franck Institute and Department of Physics, University of Chicago, Illinois 60637, USA*

(Received 13 December 2019; revised manuscript received 20 March 2020; accepted 21 April 2020; published 12 May 2020)

In the mixed-valence manganites, a near-infrared laser typically melts the orbital and spin order simultaneously, corresponding to the photoinduced $d^1d^0 \rightarrow d^0d^1$ excitations in the Mott-Hubbard bands of manganese. Here, we use ultrafast methods—both femtosecond resonant x-ray diffraction and optical reflectivity—to demonstrate that the orbital response in the layered manganite $Nd_{1-x}Sr_{1+x}MnO_4$ ($x = 2/3$) does not follow this scheme. At the photoexcitation saturation fluence, the orbital order is only diminished by a few percent in the transient state. Instead of the typical $d^1d^0 \rightarrow d^0d^1$ transition, a near-infrared pump in this compound promotes a fundamentally distinct mechanism of charge transfer, the $d^0 \rightarrow d^1L$, where L denotes a hole in the oxygen band. This finding may pave a different avenue for selectively manipulating specific types of order in complex materials of this class.

DOI: 10.1103/PhysRevB.101.201103

The correlation effect in quantum solids, which refers to the many-body interactions between charge, orbital, spin, and nuclear lattice, plays an essential role in their electronic structures, determining transport properties [1,2]. One paradigmatic example is the Mott-Hubbard insulator that dominates in the strong Coulomb repulsion ($U \rightarrow \infty$) limit, even when band theory predicts a metallic state [3]. Doping a Mott insulator with carriers often results in a rich electronic phase diagram. Notably, phase correlations lie at the heart of understanding some of the most intricate problems in quantum materials including high-temperature superconductivity [4], quantum criticality in heavy fermions systems [5], and the creation of topological states of matter driven by spin-orbit physics [6].

The mixed-valence (Mn^{3+}/Mn^{4+}) manganites promise great potential for the applications in information technology, e.g., spintronics [7] and skyrmion devices for low power consumption [8]. Fundamentally, these applications rely on the coexistence of, and interplay between, the distinct electronic orders therein [9]. On the experimental front, manipulation of the corresponding order parameters has been extensively explored from quasistatic to ultrafast time scales, using external stimuli including static magnetic [10] or electric field [11], x-ray illumination [12], as well as ultrafast optical pulses [13–19]. Under the manipulation schemes reported so far, all electronic orders will respond simultaneously to an external trigger because of the aforementioned strong correlation effect in materials of this class. For example, while a femtosecond near-infrared (NIR) pump can melt the orbital order via the resonant relaxation of the Jahn-Teller (JT) distortion, the charge and magnetic orders also collapse concomitantly [15–17]. What remains to be realized however is the essence of control in these types of quantum systems: decoupling these strong correlation effects to modify one type of order while leaving others undisturbed. This is of great importance for example for the next-generation multistate logic or memory devices [20].

*lingjias@slac.stanford.edu
†joshuat@slac.stanford.edu

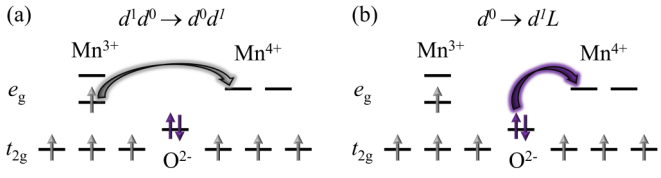

FIG. 1. Schematic view of the (a) Mott-Hubbard type $d^1d^0 \rightarrow d^0d^1$ and (b) charge-transfer type $d^0 \rightarrow d^1L$ excitations in a mixed-valence manganite.

In this Rapid Communication, we demonstrate the decoupling of strong correlations on an ultrafast time scale. We show that in a mixed-valence manganite, the orbital ordering is robust amidst intense femtosecond laser pulse excitation. This was achieved by employing resonant soft x-ray scattering (RSXS) together with optical spectroscopy to study the ultrafast dynamics in the overdoped layered system $Nd_{1-x}Sr_{1+x}MnO_4$ (NSMO, $x = 2/3$) [21]. We optically pumped the magnetic system, demonstrating a strong response within the magnetic state. We then directly studied the orbital modulation in the transient state—at the photoexcitation saturation fluence—and found an unusual resilience. That is, the RSXS intensity from the orbital order is diminished by no more than 5%. This points to the importance of the $d^0 \rightarrow d^1L$ charge-transfer photoexcitation process, where d^i $(i = 0, 1)$ and L denote the e_g orbital occupancy of the Mn^{3+}/Mn^{4+} cation and the hole in the oxygen anion band, respectively [22], and how this could be exploited to selectively control the order parameters in the transient state. This observation will be important for technological applications and draws a fundamental distinction from the $d^1d^0 \rightarrow d^0d^1$-type excitation which has been reported in past ultrafast experiments on the manganites [13–17]. This is shown schematically in Fig. 1 and will be discussed below.

A single crystal of NSMO ($x = 2/3$) was used in our study and was grown by the floating-zone method [21]. It was polished along the (110) direction. The optical conductivity ($E \parallel ab$) data were calculated by the Kramers-Kronig analysis on the reflectivity spectra measured by a combination of Fourier spectroscopy and grating spectroscopy. The NIR (1.55 eV) pump, RSXS probe measurements were performed on the SXR instrument at the Linac Coherent Light Source using the RSXS end station, an avalanche photodiode, and a recently developed THz optical system [23–26]. The pump and probe pulses propagated collinearly to the sample position with π polarization ($E_{\text{pump}} \parallel ab$). The x-ray beam energy was tuned to the Mn L_3 edge (641.5 eV) with a bandwidth of 1.3 eV [27], giving an attenuation length of about 70 nm for this geometry. The overall time resolution, calibrated by measuring the response of a sample of gallium phosphide, was about 400 fs [28]. In addition, we have performed time-resolved optical reflectivity measurements. A high-power Ti : sapphire-based laser (1.55 eV) with a 50-fs pulse duration and 120-Hz repetition rate was split and cross-polarized into the pump ($E_{\text{pump}} \parallel ab$) and probe ($E_{\text{probe}} \parallel c$) pulses, which gives a temporal resolution of about 75 fs. The optical penetration depth matches that of the x rays [29], in agreement with previous work on related systems [30].

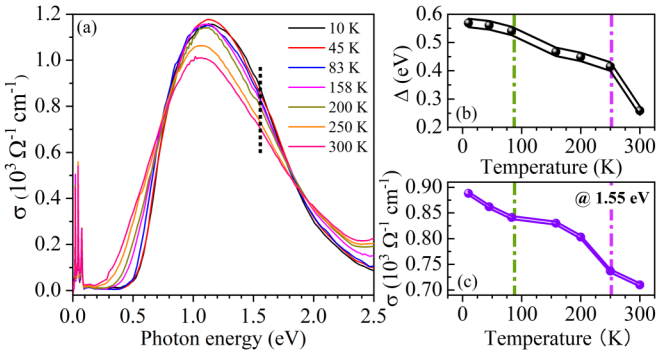

FIG. 2. (a) Optical conductivity $\sigma(\omega)$ spectra ($E \parallel ab$) of NSMO ($x = 2/3$) between 10 and 300 K. The modes below 0.1 eV come from the phonons and collective density-wave excitations [32]. The vertical dotted line marks the NIR pump energy (1.55 eV). The temperature dependencies of the optical gap (Δ) and $\sigma(\omega)$ at the NIR pump energy are shown in (b) and (c), respectively. The two dash-dotted lines mark the magnetic (90 K) and orbital (257 K) ordering temperatures [21,31,32]. Δ is calculated by a linear extrapolation of $\sigma(\omega)$ with the abscissa.

The NIR optical conductivity $\sigma(\omega)$ with $E \parallel ab$ between 10 and 300 K in the equilibrium state is shown in Fig. 2(a). A gapped mode can be clearly resolved at low temperatures. Upon heating, the optical gap Δ and conductivity $\sigma(\omega)$ at the NIR pump energy (1.55 eV) undergo a mild suppression across the antiferromagnetic (AFM) ordering temperature $T_N \simeq 90$ K [31], while a stronger one occurs around the orbital ordering temperature $T_{OO} \simeq 257$ K [Figs. 2(b) and 2(c)] [21,32]. The AFM state in this compound is of charge-exchange type and characterized by the population of zigzag ferromagnetic (FM) spin chains along the (1, 1, 0) direction [31]. As a result, the $d^1d^0 \rightarrow d^0d^1$ hopping depicted in Fig. 1(a) is plausible for the temperature dependence because it is governed by Hund's rule and short-range FM chains can persist up to T_{OO} in manganites with charge-exchange type antiferromagnetism [33]. However, the AFM state in the overdoped NSMO ($x = 2/3$) has a very short spin-correlation length along the zigzag chains, which quickly disappears around T_N [31]. From this evidence combined with the strong optical response near T_{OO}, we conclude that the NIR mode observed here is largely absent of the $d^1d^0 \rightarrow d^0d^1$ process. Indeed, the behavior revealed in Fig. 2 is characteristic of a $d^0 \rightarrow d^1L$ charge-transfer process, which gives rise to an optical gap that gets suppressed at T_{OO} due to the abrupt change in the optical spectra instead of the departure of ferromagnetism [34,35].

The ultrafast response of the optical reflectivity $R(t)$ as a function of pump fluence is shown in Fig. 3(a). These curves were fit to a single exponential decay:

$$R(t) = \frac{1}{2} \times \left[\text{erf}\left(\frac{t - t_0}{\tau_0}\right) + 1\right]\left[A_s + A_0 e^{-\left(\frac{t-t_0}{\tau_R}\right)}\right], \qquad (1)$$

where τ_0 and A_0 are the initial decay rate and amplitude, τ_R is the recovery rate of the fast component, and the constant A_s accounts for the long-lived state associated with the nuclear lattice that recovers on a much slower time scale [$\sim$400 ps at 21 mJ/cm^2, inset of Fig. 3(a)]. All the optical data presented

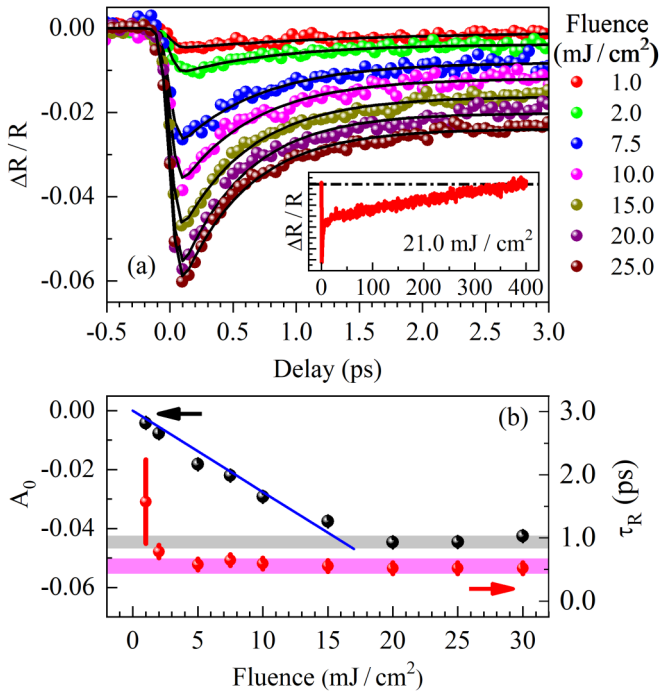

FIG. 3. (a) Temporal reflectivity change $\Delta R/R$ at 1.55 eV as a function of pump fluence (solid circles). All measurements were performed at 50 K. The solid lines are the numerical fits to Eq. (1). Inset: Measurements at 21.0 mJ/cm^2 up to 400 ps. The dash-dotted line marks the position of $\Delta R/R = 0$. (b) Fluence dependence of the initial decay amplitude A_0 (black solids, left axis) and relaxation rate (τ_R, red solids, right axis). The blue solid line is a linear fit to the A_0 data below saturation. The other solid lines are a guide to the eye.

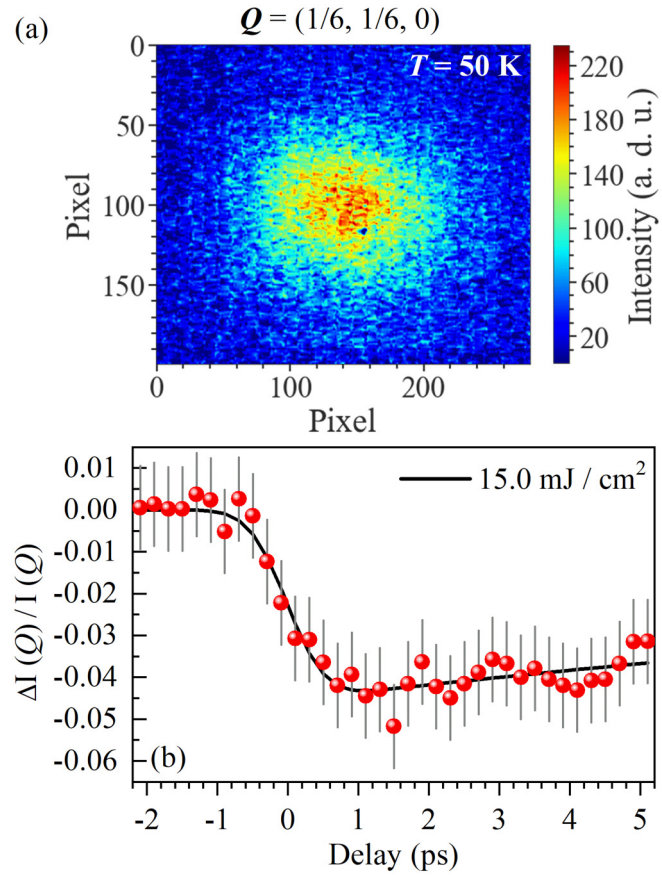

FIG. 4. (a) Background subtracted FCCD image (200 × 280 pixels) of the RSXS diffraction peak from the orbital order around $Q = (1/6, 1/6, 0)$ at 50 K. (b) Temporal evolution of the relative RSXS intensity change $[\Delta I(Q)/I(Q)]$ at $Q = (1/6, 1/6, 0)$ recorded at 50 K and 15.0 mJ / cm^2 (solid circles) by an avalanche photodiode. The solid lines are numerical fits to Eq. (1) by fixing A_s to zero.

here can be well described by Eq. (1), allowing us to quantitatively determine the electronic response to the NIR pump.

The initial reflectivity drop is always resolution-limited within the errors, i.e., $\tau_0 = 75$ fs, indicating a nonthermal excitation process. The fast recovery process is on the time scale between 0.5 and 1.0 ps [Fig. 3(b)]. This component is often assigned to the electron-electron thermalization [36] that partially recovers the electronic order [15,16]. The decay amplitude increases linearly with the fluence until saturating at 16(1) mJ/cm^2 [Fig. 3(b)]. While a NIR pump can also excite free carriers in the system, the linear fluence dependence below the saturation threshold supports the notion that the pump induced reflectivity change at 1.55 eV must mainly come from the above-the-band-gap electronic excitations [15,30,32,37]. This is supported by the strongly gapped optical mode [Fig. 2(a)]. As a result, our optical data have revealed that the electronic system has been saturated by the femtosecond NIR pump at $f_{sat} = 16(1)$ mJ/cm^2, through the ultrafast $d^0 \rightarrow d^1\underline{L}$ charge-transfer process [Fig. 1(b)].

Typically, the ultrafast dynamics in a manganite under an optical pump are governed by the Mott-Hubbard type $d^1d^0 \rightarrow d^0d^1$ excitations. This strongly suppresses the underlying orbital order, as has been reported by many authors [13–17]. We implemented RSXS to investigate if the ultrafast orbital order response is consistent with a charge-transfer-type excitation.

Figure 4(a) shows the RSXS diffraction image around $Q = (1/6, 1/6, 0)$ recorded by the FCCD detector at 50 K. This position was chosen because the modulation vector of the orbital order in materials of this class is predicted to be $\boldsymbol{k} = (\delta, \delta, 0)$, where δ is determined by the hole concentration: $\delta \approx (1 - x)/2$ [21]. In the NSMO family, an incommensurate superlattice at this position has been observed by electron diffraction [21], but it has never been directly verified which states contribute to this superstructure. Since resonant scattering at the L edge probes the unoccupied d-orbital state, this first of all directly confirms that the modulation is driven by the Mn d-orbital states.

Next the ultrafast dynamics of the orbital order under femtosecond NIR excitation were measured. For 15.0 mJ/cm^2, which is slightly below or equal to f_{sat} [Fig. 3(b)], the RSXS pump-probe curve is shown in Fig. 4(b). This behavior also fits well to Eq. (1). The initial x-ray-scattering intensity decay is resolution limited, but is given here by the jitter of the optical and x-ray pulse arrival time, i.e., $\tau_0 = 400$ fs [38]. This verifies the nonthermal nature of this photoinduced transition.

For recovery times, the time window is not wide enough to reliably fit the A_s term on the longer time scales. Fixing it to zero leads to $\tau_R = 23(7)$ ps. This value is smaller than the spin-lattice thermalization, i.e., the energy transfer from the initially excited electron system to the nuclear lattice; this time scale is usually long (> 100 ps) in relevant systems [30]. But τ_R is also considerably longer than the fast electronic recovery process extracted from the optical reflectivity measurements [$\leqslant 1.0$ ps, Fig. 3(b)]. This intermediate recovery process, which has been observed in other nonoptimally doped manganites [16], is related to the transient photoinduced phase separation that leads to an inhomogeneous recovery of the electronic order. There seems to be evidence of an oscillation immediately after the pumped orbital state, but as this frequency is much longer than the typical phonon modes found in relevant systems [15,19,39], we believe it is unlikely to be real orbital excitations.

Most importantly, we have found that the orbital order is surprisingly robust against this photoexcitation. Although the electronic system is saturated by the NIR pump at 15.0 mJ/cm^2 [Fig. 3(b)], the RSXS intensity scattered by the orbital order is only suppressed by about between 4% and 5% in the transient state. Because we have carefully calibrated the energy density for the different geometries and experiments, this character sharply contrasts the observations in other manganites [29]. In previous experiments on similar systems, the same NIR excitation promotes the Mott-Hubbard type $d^1d^0 \rightarrow d^0d^1$ transitions [Fig. 1(a)] and therefore greatly suppresses the underlying orbital order [15].

According to the Zaanen-Sawatzky-Allen classification scheme, the electronic structure near the Fermi surface (FS) of a correlated transition-metal insulator depends on not only the Hubbard U, but also on the charge-transfer energy Δ [22]. Due to the comparable U and Δ values in mixed-valence manganites, the above-the-band-gap excitation near the FS can to be dominated by either the $d^1d^0 \rightarrow d^0d^1$ transition, the $d^0 \rightarrow d^1L$, or both [40–43]. Our RSXS observations rule out a meaningful contribution from the former in NSMO ($x = 2/3$), since the relative orbital order intensity loss of no more than 5% in the transient state is measured close to f_{sat}. On the other hand, the d^1L transient state created by the charge-transfer process does not contribute to ordered orbital structure because of the twofold e_g degeneracy [44]. Consequently, the bulk orbital order structure would not be expected to change considerably under this photoexcitation scheme. The robustness of the orbital order therefore strongly indicates that the latter charge-transfer type scheme is responsible for the NIR photoexcitation process in this compound [Fig. 1(b)]. This is consistent with the temperature dependence of the optical spectrum at these energies (Fig. 2).

To obtain more insight about the nature of the large optical spectral weight at 1.55 eV in Fig. 2(a), we measured the ultrafast dynamics of the optical reflectivity at 15 mJ/cm^2 as a function of temperature (Fig. 5). The decay amplitude A_0 changes smoothly with temperature below about T_N. Upon further heating, A_0 is suppressed and falls below the noise level around 110 K [Fig. 5(b)]. This suggests that the electronic excitation process triggered by the NIR pump here is magnetically activated: the increased probability amplitude for the hopping matrix element—only in the magnetic state—

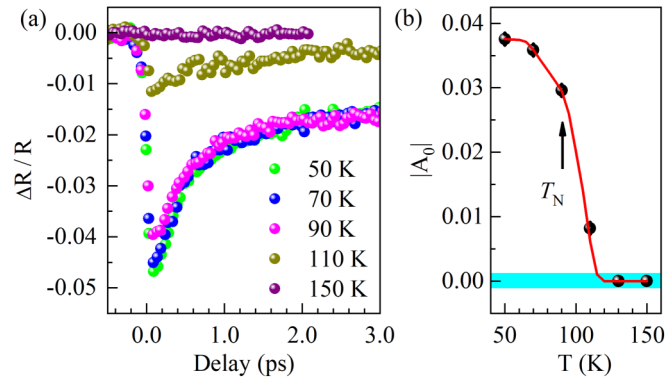

FIG. 5. (a) Temporal evolution of the relative optical reflectivity change ($\Delta R/R$) as a function of temperature. All the curves were recorded at the pump fluence 15 mJ/cm^2. (b) Temperature dependence of the absolute value of the initial decay amplitude (A_0) extracted from Eq. (2) (solid circles). The red line and shaded area are guides for the eye.

originates from the hybridized wave function. Intuitively, this character does not fit the $d^0 \rightarrow d^1L$ scenario depicted in Fig. 1(b) because it does not require magnetic order. However, similar behavior is expected if the e_g band formed by the Mn^{3+} cations is involved. For example, the $d^1d^0 \rightarrow d^0d^1$ process in Fig. 1(a) belongs to this category; it is energetically favored if the adjacent Mn^{3+}/Mn^{4+} spins are parallel with each other, a configuration that is only fulfilled in the magnetically ordered region of the relevant manganites [15,17,30].

Since the orbital response and optical spectroscopy imply the $d^1d^0 \rightarrow d^0d^1$ contribution is very weak in NSMO ($x = 2/3$), we propose that the $d^0 \rightarrow d^1L$ process is between the hybridized Mn ($3d$) and O ($2p$) bands near the FS [32]. The dp hybridization occurs when U and Δ are similar in strength [41,42]. In this modified scenario, the O^{2-} $2p$ electrons are spin polarized by the $Mn^{3+}e_g$ electrons in the hybridized dp band. Accordingly, the photoinduced charge transfer is allowed along the FM zigzag spin chains along the (1, 1, 0) direction, which is restricted in the AFM state of NSMO ($x = 2/3$) [31]. This scenario naturally explains the ultrafast results presented here as well as the mild change in the static NIR optical spectrum around T_N (Fig. 2).

Furthermore, the $d^0 \rightarrow d^1L$ scenario may also be partially responsible for the ultrafast orbital dynamics in the other layered manganite $La_{1-x}Sr_{1+x}MnO_4$ ($x = 1/2$) [30]. In this compound, a femtosecond NIR pump melts about 25% of the orbital order reflection probed by RSXS at the saturation fluence, whereas the AFM order is completely suppressed. This finite RSXS intensity was explained by the residual JT distortion after the photoexcitation [30]. A recent femtosecond NIR pump/hard x-ray probe work on $Pr_{1-x}Ca_xMnO_3$ ($x = 1/2$), where the $d^1d^0 \rightarrow d^0d^1$ physics is clearly dominant, directly revealed that the JT distortion disappears with the orbital and charge order when the electronic system is fully excited [15] and therefore does not fit the model proposed in Ref. [30]. Alternatively, the residual orbital order in $La_{1-x}Sr_{1+x}MnO_4$ ($x = 1/2$) could indicate that about 75% of the electronic excitations involve the $d^0 \rightarrow d^1L$ charge transfer.

In conclusion, we have investigated the effect of NIR excitation (1.55 eV) on the orbital order in the layered manganite NSMO ($x = 2/3$) through ultrafast techniques. Conducting a systematic ultrafast optical reflectivity study, we found the fluence and temperature dependence of the optical reflectivity change. By using RSXS at an x-ray free-electron laser source, we combined this finding with the ability to directly monitor the femtosecond orbital response in the transient photoexcited state. We found that the RSXS intensity arising from the orbital order is diminished by no more than 5% percent while the electronic system is fully saturated. These results strongly suggest that the photoexcitation mechanism in this compound is $d^0 \rightarrow d^1L$, instead of the commonly assumed $d^1d^0 \rightarrow d^0d^1$. In addition, we show that the correct description of the photoexcitation process requires the dp hybridization near the FS in the magnetically ordered state. Taking advantage of the hybridized $d^0 \rightarrow d^1L$ charge-transfer mechanism holds great potential for selectively manipulating the electronic order. Furthermore, this shows that other excitation mechanisms at play may be more closely related to that seen in the cuprates, such as the high-energy scale physics associated with Mott-like excitations [45]. The results here point to future work based on exploiting the different transfer mechanisms for specific materials to unravel the emergent excitations in systems with multiple types of order, especially other quantum materials that display nearly degenerate energy scales, such as multiferroics [20].

We acknowledge useful discussions with R. Schoenlein, A. Sakdinawat, S. Johnson, and U. Staub. Special thanks to D. Green, K. Thompson, and S. Curry. We are grateful for data support from J. Thayer and C. O'Grady. This work was supported by the U. S. Department of Energy, Office of Science, Basic Energy Sciences, Materials Sciences and Engineering Division, under Contract No. DE-AC02-76SF00515. The use of the Linac Coherent Light Source (LCLS), SLAC National Accelerator Laboratory, was also supported under the same contract. Y-D.C. acknowledges the support from the Advanced Light Source, a DOE Office of Science User Facility under Contract No. DE-AC02-05CH11231. J.J.T. acknowledges support from the U.S. DOE, Office of Science, Basic Energy Sciences through the Early Career Research Program.

[1] E. Dagotto, Rev. Mod. Phys. **66**, 763 (1994).
[2] E. Dagotto, Science **309**, 257 (2005).
[3] N. F. Mott, Proc. Phys. Soc., Sec. A **62**, 416 (1949).
[4] B. Keimer, S. A. Kivelson, M. R. Norman, S. Uchida, and J. Zaanen, Nature (London) **518**, 179 (2015).
[5] Q. Si and F. Steglich, Science **329**, 1161 (2010).
[6] J. G. Rau, E. K.-H. Lee, and H.-Y. Kee, Annu. Rev. Condens. Matter Phys. **7**, 195 (2016).
[7] M. Bibes and A. Barthelemy, IEEE Trans. Electron Devices **54**, 1003 (2007).
[8] X. Z. Yu, Y. Tokunaga, Y. Kaneko, W. Z. Zhang, K. Kimoto, Y. Matsui, Y. Taguchi, and Y. Tokura, Nat. Commun. **5**, 3198 (2014).
[9] E. Dagotto, T. Hotta, and A. Moreo, Phys. Rep. **344**, 1 (2001).
[10] S. Yamada, N. Abe, H. Sagayama, K. Ogawa, T. Yamagami, and T. Arima, Phys. Rev. Lett. **123**, 126602 (2019).
[11] A. S. Dhoot, C. Israel, X. Moya, N. D. Mathur, and R. H. Friend, Phys. Rev. Lett. **102**, 136402 (2009).
[12] V. Kiryukhin, D. Casa, J. P. Hill, B. Keimer, A. Vigliante, Y. Tomioka, and Y. Tokura, Nature (London) **386**, 813 (1997).
[13] M. Matsubara, Y. Okimoto, T. Ogasawara, Y. Tomioka, H. Okamoto, and Y. Tokura, Phys. Rev. Lett. **99**, 207401 (2007).
[14] T. Li, A. Patz, L. Mouchliadis, J. Yan, T. A. Lograsso, I. E. Perakis, and J. Wang, Nature (London) **496**, 69 (2013).
[15] P. Beaud, A. Caviezel, S. O. Mariager, L. Rettig, G. Ingold, C. Dornes, S.-W. Huang, J. A. Johnson, M. Radovic, T. Huber, T. Kubacka, A. Ferrer, H. T. Lemke, M. Chollet, D. Zhu, J. M. Glownia, M. Sikorski, A. Robert, H. Wadati, M. Nakamura *et al.*, Nat. Mater. **13**, 923 (2014).
[16] M. C. Langner, S. Zhou, G. Coslovich, Y.-D. Chuang, Y. Zhu, J. S. Robinson, W. F. Schlotter, J. J. Turner, M. P. Minitti, R. G. Moore, W. S. Lee, D. H. Lu, D. Doering, P. Denes, Y. Tomioka, Y. Tokura, R. A. Kaindl, and R. W. Schoenlein, Phys. Rev. B **92**, 155148 (2015).
[17] S. Y. Zhou, M. C. Langner, Y. Zhu, Y.-D. Chuang, M. Rini, T. E. Glover, M. P. Hertlein, A. G. C. Gonzalez, N. Tahir, Y. Tomioka, Y. Tokura, Z. Hussain, and R. W. Schoenlein, Sci. Rep. **4**, 4050 (2014).
[18] M. Först, C. Manzoni, S. Kaiser, Y. Tomioka, Y. Tokura, R. Merlin, and A. Cavalleri, Nat. Phys. **7**, 854 (2011).
[19] M. Porer, L. Rettig, E. M. Bothschafter, V. Esposito, R. B. Versteeg, P. H. M. van Loosdrecht, M. Savoini, J. Rittmann, M. Kubli, G. Lantz, O. J. Schumann, A. A. Nugroho, M. Braden, G. Ingold, S. L. Johnson, P. Beaud, and U. Staub, Phys. Rev. B **101**, 075119 (2020).
[20] N. A. Spaldin and R. Ramesh, Nat. Mater. **18**, 203 (2019).
[21] T. Kimura, K. Hatsuda, Y. Ueno, R. Kajimoto, H. Mochizuki, H. Yoshizawa, T. Nagai, Y. Matsui, A. Yamazaki, and Y. Tokura, Phys. Rev. B **65**, 020407(R) (2001).
[22] J. Zaanen, G. A. Sawatzky, and J. W. Allen, Phys. Rev. Lett. **55**, 418 (1985).
[23] G. L. Dakovski, P. Heimann, M. Holmes, O. Krupin, M. P. Minitti, A. Mitra, S. Moeller, M. Rowen, W. F. Schlotter, and J. J. Turner, J. Synchrotron Radiat. **22**, 498 (2015).
[24] C. Bostedt, S. Boutet, D. M. Fritz, Z. Huang, H. J. Lee, H. T. Lemke, A. Robert, W. F. Schlotter, J. J. Turner, and G. J. Williams, Rev. Mod. Phys. **88**, 015007 (2016).
[25] D. Doering, Y. D. Chuang, N. Andresen, K. Chow, D. Contarato, C. Cummings, E. Domning, J. Joseph, J. S. Pepper, B. Smith *et al.*, Rev. Sci. Instrum. **82**, 073303 (2011).
[26] J. J. Turner, G. L. Dakovski, M. Hoffmann, H. Y. Hwang, A. Zarem, W. F. Schlotter, S. Moeller, M. P. Minitti, U. Staub, S. Johnson *et al.*, J. Synchrotron Radiat. **22**, 621 (2015).
[27] K. Tiedtke, A. A. Sorokin, U. Jastrow, P. Juranic, S. Kreis, N. Gerken, M. Richter, U. Arp, Y. Feng, and D. Nordlund, Opt. Express **22**, 21214 (2014).
[28] O. Krupin, M. Trigo, W. F. Schlotter, M. Beye, F. Sorgenfrei, J. J. Turner, D. A. Reis, N. Gerken, S. Lee, W. S. Lee *et al.*, Opt. Express **20**, 11396 (2012).
[29] We have carefully calculated the refractive index at the NIR pump energy based on the optical conductivity [Fig. 1(c)] to obtain a value of 2.62, giving a penetration depth of 67 nm.

This value was then used for the energy density calculation. The incident pump angles in different geometries have also been taken into account, producing internal angles leading only to small corrections of the energy density value (<10%), within the energy density errors.

[30] H. Ehrke, R. I. Tobey, S. Wall, S. A. Cavill, M. Först, V. Khanna, T. Garl, N. Stojanovic, D. Prabhakaran, A. T. Boothroyd, M. Gensch, A. Mirone, P. Reutler, A. Revcolevschi, S. S. Dhesi, and A. Cavalleri, Phys. Rev. Lett. **106**, 217401 (2011).

[31] H. Ulbrich, P. Steffens, D. Lamago, Y. Sidis, and M. Braden, Phys. Rev. Lett. **108**, 247209 (2012).

[32] J. Fujioka, Y. Ida, Y. Takahashi, N. Kida, R. Shimano, and Y. Tokura, Phys. Rev. B **82**, 140409(R) (2010).

[33] R. Kajimoto, T. Kakeshita, Y. Oohara, H. Yoshizawa, Y. Tomioka, and Y. Tokura, Phys. Rev. B **58**, R11837 (1998).

[34] K. Tobe, T. Kimura, Y. Okimoto, and Y. Tokura, Phys. Rev. B **64**, 184421 (2001).

[35] N. N. Kovaleva, A. V. Boris, C. Bernhard, A. Kulakov, A. Pimenov, A. M. Balbashov, G. Khaliullin, and B. Keimer, Phys. Rev. Lett. **93**, 147204 (2004).

[36] R. D. Averitt and A. J. Taylor, J. Phys.: Condens. Matter **14**, R1357 (2002).

[37] V. Esposito, L. Rettig, E. Abreu, E. M. Bothschafter, G. Ingold, M. Kawasaki, M. Kubli, G. Lantz, M. Nakamura, J. Rittman, M. Savoini, Y. Tokura, U. Staub, S. L. Johnson, and P. Beaud, Phys. Rev. B **97**, 014312 (2018).

[38] M. Beye, O. Krupin, G. Hays, A. H. Reid, D. Rupp, S. d. Jong, S. Lee, W. S. Lee, Y. D. Chuang, R. Coffee *et al.*, Appl. Phys. Lett. **100**, 121108 (2012).

[39] R. Singla, A. Simoncig, M. Först, D. Prabhakaran, A. L. Cavalieri, and A. Cavalleri, Phys. Rev. B **88**, 075107 (2013).

[40] T. Arima, Y. Tokura, and J. B. Torrance, Phys. Rev. B **48**, 17006 (1993).

[41] A. Gössling, M. W. Haverkort, M. Benomar, H. Wu, D. Senff, T. Möller, M. Braden, J. A. Mydosh, and M. Grüninger, Phys. Rev. B **77**, 035109 (2008).

[42] S. Mildner, J. Hoffmann, P. E. Blöchl, S. Techert, and C. Jooss, Phys. Rev. B **92**, 035145 (2015).

[43] R. Kraus, M. Schrade, R. Schuster, M. Knupfer, A. Revcolevschi, B. Büchner, and J. Geck, Phys. Rev. B **83**, 165130 (2011).

[44] In the case of a transient JT distortion on the e_g orbitals that are degenerate in equilibrium, no additional long-range orbital order can be probed on the femto- to picosecond time scale because the formation of its spatial coherence is limited by the speed of sound [15].

[45] C. Giannetti, F. Cilento, S. D. Conte, G. Coslovich, G. Ferrini, H. Molegraaf, M. Raichle, R. Liang, H. Eisaki, M. Greven, A. Damascelli, D. van der Marel, and F. Parmigiani, Nat. Commun. **2**, 353 (2011).